International Journal for Housing Science and Its Applications

Publish September 16, 2025. Volume 47, Issue 1 Pages 1150-1158

https://doi.org/10.70517/ijhsa47199

Meta-Spectral Net: Meta-Learning Framework for Adaptive Spectral Variability Modeling in Hyperspectral Unmixing

Jirui Liu[1], Jinhui Lan[1,*] and Liu wenbing[1]

[1] the school of Automation and Electrical Engineering, University of Science and Technology Beijing, Beijing, China

Corresponding authors: (e-mail: lanjh@ustb.edu.cn).

Abstract Spectral variability remains a major challenge in hyperspectral unmixing, as the spectral signatures of the same material often fluctuate under different illumination, atmospheric, or scale conditions, which invalidates the fixed endmember assumption. To address this issue, we propose Meta-Spectral Net, a meta-learning-based framework for adaptive spectral variability modeling in hyperspectral unmixing. The proposed framework leverages a task-driven meta-learning strategy, where each acquisition scenario is defined as a task, to enable the endmember generator to rapidly adapt to unseen spectral conditions with only a few samples. Furthermore, a spectral variability adaptation module is introduced to explicitly account for environmental factors, thus improving the robustness of endmember representation. Comprehensive experiments on both synthetic and real hyperspectral datasets demonstrate that Meta-Spectral Net significantly outperforms state-of-the-art unmixing methods in terms of endmember reconstruction accuracy and abundance estimation, while offering superior generalization to novel scenarios. These results suggest that meta-learning provides an effective paradigm for tackling spectral variability, paving the way toward more adaptive and reliable hyperspectral unmixing in real-world applications.

Index Terms hyperspectral unmixing, spectral variability, meta-learning, adaptive modeling, endmember generation

I. Introduction

Hyperspectral remote sensing (HRS), which integrates imaging and spectroscopy, has emerged as a powerful technology for Earth observation. By capturing reflectance information across hundreds of contiguous narrow spectral bands, HRS enables fine-grained identification and analysis of material composition, and thus plays a crucial role in applications such as precision agriculture, mineral exploration, and environmental monitoring [1]–[3]. However, due to the limited spatial resolution of hyperspectral sensors, each pixel often contains a mixture of multiple materials, and its spectral response is a combination of these constituent signatures. To extract physically meaningful information, hyperspectral unmixing (HSU) has become an essential technique for estimating the spectral signatures of pure materials, known as endmembers, as well as their fractional abundances [4]–[6].

Among existing models, the Linear Mixing Model (LMM) has been widely adopted due to its simplicity and interpretability. The LMM assumes that each observed spectrum is a convex combination of endmembers, with abundance coefficients subject to non-negativity and sum-to-one constraints. Nevertheless, in practice, this assumption often fails because of a critical challenge: spectral variability. The spectral signatures of the same material may vary significantly under different illumination conditions, atmospheric effects, moisture levels, or scale differences [7]–[9]. Such variability leads to discrepancies between the observed spectra and the assumed fixed endmembers, thereby degrading the performance of traditional LMM-based approaches.

To mitigate spectral variability, a variety of approaches have been explored.

(1) Parameterized endmember models, such as the Perturbed Endmember Model (PEMM) and the Extended LMM (ELMM), explicitly introduce transformations to capture spectral shifts. However, they remain limited in handling complex, nonlinear variability caused by coupled environmental factors [10].

(2) Deep generative models, such as Variational Autoencoders (VAEs) and Generative Adversarial Networks (GANs), attempt to learn the latent distribution of endmembers and generate variable spectra [11], [12]. While promising, these approaches typically require large-scale training data and show limited generalization to unseen scenarios.

(3) Spectral library-based methods leverage large collections of reference endmembers to represent variability [13]. Yet, these methods face challenges in computational efficiency and stability when dealing with high-dimensional libraries.

Despite these advances, three major challenges remain unresolved:

(1)Limited adaptability: Most existing methods are trained on specific datasets and lack the flexibility to adapt to new acquisition conditions.

(2)Strong data dependency: Deep learning-based approaches rely heavily on abundant annotated samples, which are often scarce in remote sensing applications.

(3)Weak generalization: Models trained in one environment frequently fail to transfer to different sensors, regions, or acquisition conditions.

Recently, meta-learning has gained attention as an effective paradigm for few-shot learning and rapid adaptation. By training across a distribution of tasks, meta-learning enables models to learn transferable knowledge and adapt quickly to new tasks with minimal samples [14], [15]. This paradigm is particularly well-suited for hyperspectral unmixing under spectral variability: each acquisition scenario can be regarded as a distinct task, and a meta-learned unmixing model can adapt its endmember representation efficiently to new conditions.

Motivated by this, we propose Meta-Spectral Net, a meta-learning-based framework for adaptive spectral variability modeling in hyperspectral unmixing. The key contributions of this work are summarized as follows:

Meta-learning framework for adaptive unmixing: We formulate spectral variability as a task distribution and employ meta-learning to enable rapid adaptation of endmember representations to novel scenes with few samples.

Spectral variability adaptation module: We design an explicit module to incorporate environmental factors such as illumination, atmospheric effects, and scale, thereby enhancing the robustness and physical interpretability of endmember modeling.

Comprehensive experimental validation: We conduct extensive experiments on both synthetic and real hyperspectral datasets, comparing our method with state-of-the-art baselines. Results demonstrate that Meta-Spectral Net achieves superior performance in both endmember reconstruction and abundance estimation, while exhibiting stronger generalization to unseen scenarios.

The remainder of this paper is organized as follows. Section 2 reviews related work on hyperspectral unmixing and spectral variability modeling. Section 3 introduces the proposed Meta-Spectral Net framework. Section 4 presents the experimental setup and results. Section 5 provides discussion and analysis. Finally, Section 6 concludes the paper and outlines future research directions.

II. Related Work

II. A. Hyperspectral Unmixing Models

Hyperspectral unmixing (HSU) has been extensively studied over the past two decades and can be broadly categorized into geometrical, statistical, and sparse regression-based approaches [1], [4]. Among them, the Linear Mixing Model (LMM) has been the most widely adopted due to its mathematical simplicity and physical interpretability 2,5. The LMM assumes that each observed spectrum is a linear convex combination of endmembers with non-negative abundance fractions. Various algorithms, such as Vertex Component Analysis (VCA), Nonnegative Matrix Factorization (NMF), and sparse unmixing, have been developed under the LMM framework [4], [13].

However, real-world mixing processes are often more complex, and linear assumptions fail in many cases. This has motivated the development of Nonlinear Mixing Models (NLMMs) [8], [9], which account for multiple scattering, intimate mixtures, or nonlinear interactions between materials. Representative nonlinear models include the bilinear model, the polynomial post-nonlinear model, and kernel-based approaches. While NLMMs can better capture physical reality, they typically require more parameters, leading to increased computational complexity and reduced robustness in large-scale applications.

II. B. Spectral Variability Modeling

Spectral variability refers to the phenomenon that the same material exhibits different spectral responses under varying acquisition conditions, such as illumination geometry, atmospheric effects, seasonal changes, or scale differences. Addressing spectral variability has become a central issue in hyperspectral unmixing research [5]–[7].

To cope with this challenge, several strategies have been proposed: Parameterized Endmember Models: Models such as the Perturbed Endmember Model (PEMM) and the Extended Linear Mixing Model (ELMM) introduce parametric transformations to capture endmember variability [7], [10]. Although effective in simple cases, these models are often limited in representing highly nonlinear or coupled variations. Spectral Library-Based Approaches: By employing large spectral libraries, these methods attempt to represent material variability through a wide range of candidate endmembers [13]. However, the large search space brings significant computational burden, and selecting the most representative subset remains challenging. Deep Generative Models: Inspired by advances in machine learning, methods based on Variational Autoencoders (VAEs) and Generative Adversarial Networks (GANs) have been proposed to learn the latent distributions of endmembers and generate spectrally diverse samples [11], [12]. These models have shown improved flexibility, but they require abundant training data and often suffer from poor generalization to unseen conditions.

Despite these developments, most existing approaches exhibit limited adaptability and fail to generalize well across different sensors, regions, or acquisition scenarios. This motivates the exploration of new learning paradigms capable of addressing spectral variability in a more flexible and robust manner.

II. C. Meta-Learning and Adaptive Learning in Remote Sensing

Meta-learning, also known as "learning to learn," has recently emerged as a powerful paradigm for few-shot learning and rapid adaptation [14], [15]. Unlike conventional deep learning, which focuses on minimizing task-specific loss functions, meta-learning aims to extract transferable knowledge across a distribution of tasks. By doing so, a model can adapt to new tasks with only a few labeled samples. The Model-Agnostic Meta-Learning (MAML) framework [14] and its variants have demonstrated significant success in computer vision, natural language processing, and reinforcement learning.

In the field of remote sensing, meta-learning has been applied to tasks such as hyperspectral image classification, land cover mapping, and object detection, where data scarcity and domain shifts are common challenges. Studies have shown that meta-learning can effectively reduce the dependency on large-scale annotated datasets and improve cross-domain generalization. However, its application to hyperspectral unmixing, particularly in modeling spectral variability, remains largely unexplored.

Given that spectral variability can be naturally viewed as a distribution of tasks across different acquisition conditions, meta-learning provides a promising avenue for developing adaptive unmixing methods. By treating each scene as a task and leveraging few-shot adaptation, meta-learning-based frameworks could enable robust modeling of spectral variability without requiring extensive retraining or large annotated datasets.

III. Proposed Method

In this section, we present the proposed Meta-Spectral Net framework, which integrates meta-learning with adaptive spectral variability modeling for hyperspectral unmixing. The framework consists of three components: (1) a task-oriented unmixing formulation under spectral variability; (2) a meta-learning strategy for endmember adaptation; and (3) an abundance estimation module (Figure 1).

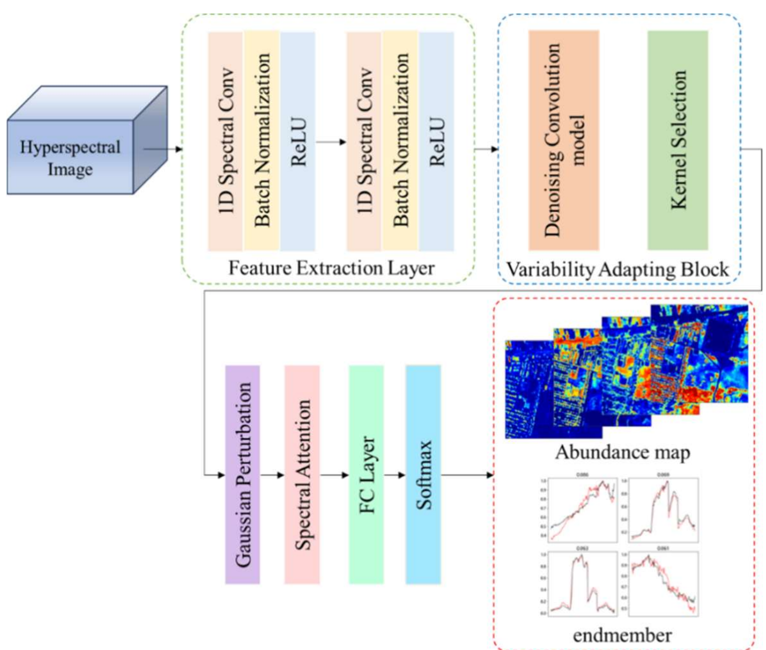

Figure 1: Network Structure Diagram

III. A. Problem Formulation

Let $Y \in R^{L \times N}$ denote a hyperspectral image, where L is the number of spectral bands and N is the number of pixels. The classical Linear Mixing Model (LMM) represents each pixel spectrum $y_n \in R^L$ *as*:

$$y_n = Ma_n + e_n, \forall n \in \{1, \dots, N\} \quad (1)$$

where $M \in R^{L \times K}$ denotes the matrix of K endmember signatures, $a_n \in R^K$ denotes the abundance vector, and e_n is the reconstruction error subject to constraints:

$$a_{kn} \geq 0, \sum_{k=1}^{K} a_{kn} = 1 \tag{2}$$

However, due to spectral variability, the fixed endmember matrix M becomes inadequate. Instead, we introduce an adaptive endmember model:

$$y_n = M(\theta_n)a_n + e_n \tag{3}$$

where $M(\theta_n)$denotes the parameterized endmember set adapted by variability factor θ_n. The challenge is to estimate both θ_n and a_n efficiently across diverse acquisition conditions.

III. B. Meta-Learning Framework

We formulate spectral variability modeling as a meta-learning problem. Each hyperspectral scene is regarded as a task $\mathcal{T}_i$ defined by:

$$\mathcal{T}_i = \{Y_i, A_i\} \tag{4}$$

where Y_i and A_i denote the observed spectra and corresponding abundances.

During training, we optimize for a set of meta-parameters ϕ that serve as an initialization for endmember estimation. For each task $\mathcal{T}_i$ the model undergoes inner-loop adaptation:

$$\phi' = \phi - \alpha\nabla_{\phi}\mathcal{L}_{\mathcal{T}_i}(\phi) \tag{5}$$

where α is the inner learning rate and $\mathcal{L}_{\mathcal{T}_i}$ is the reconstruction loss under task $\mathcal{T}_i$

$$\mathcal{L}_{\mathcal{T}_i} = \frac{1}{N_i}\sum_{n=1}^{N_i} |y_{in} - M(\phi)a_{in}|_2^2 \tag{6}$$

The outer-loop meta-update is then computed across tasks:

$$\phi \leftarrow \phi - \beta\nabla_{\phi}\sum_{i}\mathcal{L}_{\mathcal{T}_i}(\phi') \tag{7}$$

where β is the outer learning rate. This bi-level optimization enables the model to learn a robust initialization that can rapidly adapt to unseen variability with only a few samples.

III. C. Abundance Estimation with Adaptive Endmembers

Once the task-specific endmember set $M(\theta)$ is obtained through meta-adaptation, the abundance estimation is formulated as a constrained optimization problem:

$$\widehat{a_n} = \arg\min_{a_n} |y_n - M(\theta)a_n|_2^2 \tag{8}$$

subject to:

$$a_{kn} \geq 0, \quad \sum_{k=1}^{K} a_{kn} = 1 \tag{9}$$

We solve this optimization using projected gradient descent (PGD), ensuring feasibility under the simplex constraints.

III. D. Algorithm Summary

The overall procedure of Meta-Spectral Net is summarized in Algorithm 1.

Algorithm 1: Meta-Spectral Net for Hyperspectral Unmixing

1. Input: Training tasks \{T_i \}, learning rates α,β.
2. Initialize meta-parameters ϕ.
3. For each iteration:

Sample batch of tasks$\mathcal{T}_i$.

For each task:

Compute adapted parameters $\phi' = \phi - \alpha\nabla_{\phi}\mathcal{L}_{\mathcal{T}_i}(\phi)$.

Meta-update: $\phi \leftarrow \phi - \beta\nabla_{\phi}\mathcal{L}_{\mathcal{T}_i}(\phi')$.

4. Output: Meta-learned initialization ϕ.

III. E. Hyperparameter Configuration

Table 1 summarizes the hyperparameters used in our framework.

Table 1: Hyperparameter settings of Meta-Spectral Net

Hyperparameter	Description	Value / Range
K	Number of endmembers	3–10 (dataset dependent)
L	Number of spectral bands	100–224 (dataset dependent)
α	Inner-loop learning rate	1×10^{-3}
β	Outer-loop learning rate	5×10^{-4}
Inner steps	Number of inner-loop updates per task	5
Outer steps	Number of meta-update iterations	10,000
Batch size	Number of tasks per meta-update	8
Optimizer	Optimization algorithm	Adam
Stopping criterion	Convergence of validation loss	Early stopping (patience = 20)

IV. Experiments and Results

This section presents a comprehensive evaluation of the proposed Meta-Spectral Net framework, assessing its performance in hyperspectral unmixing across three widely adopted benchmark datasets: Urban, Samson, and Moffett. We begin by detailing the experimental setup, including descriptions of the datasets, the state-of-the-art methods used for comparison, and the evaluation metrics employed. This is followed by a presentation and in-depth discussion of both quantitative results and qualitative findings, analyzing the model's efficacy in spectral reconstruction and abundance estimation.

IV. A. Experimental Setup

The experiments were conducted on three real-world hyperspectral scenes, each presenting distinct unmixing challenges. The Urban dataset, captured by the HYDICE sensor over an urban environment, comprises 162 spectral bands following the removal of water absorption bands. This scene features a complex mixture of man-made structures and natural materials, with four predominant endmembers: Asphalt, Grass, Tree, and Roof. The Samson dataset consists of 156 spectral bands and a spatial resolution of 95×95 pixels. It serves as a standard benchmark for smaller-scale unmixing tasks and is characterized by three primary endmembers: Soil, Tree, and Water. The Moffett dataset contains 187 spectral bands with a spatial size of 100×100 pixels. This scene is particularly notable for exhibiting strong spectral variability, largely influenced by varying water content and coastal effects, and contains three principal endmembers: Soil, Vegetation, and Water.

To ensure a rigorous and fair comparison, the performance of Meta-Spectral Net was evaluated against six representative unmixing approaches, spanning classical geometric, statistical, and deep learning-based methods. These include: Non-negative Matrix Factorization (NMF)[16], a foundational statistical approach; NMF with Spectral Variability modeling (NMF-SV)[17], which extends NMF to account for variability; the Perturbed Linear Mixing Model (PLMM)[7], a parametric model designed for endmember variability; and GAN-HU[18], a method leveraging Generative Adversarial Networks for hyperspectral unmixing.

A comprehensive assessment was performed using three complementary metrics to evaluate different aspects of unmixing performance. The Spectral Angle Distance (SAD) was used to measure the spectral fidelity between the estimated and reference endmembers, with lower values indicating higher spectral similarity. The accuracy of the estimated fractional abundances was quantified using the Root Mean Square Error (RMSE). Furthermore, the overall fidelity of the reconstructed hyperspectral scene was evaluated using the Reconstruction Error (RE), which calculates the root mean square error between the original and the reconstructed pixels.

IV. B. Quantitative Results

The quantitative performance of the proposed Meta-Spectral Net and all baseline methods across the Urban, Samson, and Moffett datasets is comprehensively summarized in Tables 2 to 4. The results demonstrate a consistent and superior performance of our method over all competing approaches on every dataset.

Table 2: Quantitative results on the Urban dataset

Method	SAD	RMSE	RE
NMF	0.121	0.055	0.042
NMF-SV	0.112	0.048	0.039
PLMM	0.108	0.046	0.037
GAN-HU	0.093	0.041	0.032
Meta-Spectral Net (Ours)	0.082	0.036	0.028

Table 3: Quantitative results on the Samson dataset

Method	SAD	RMSE	RE
NMF	0.115	0.048	0.038
NMF-SV	0.106	0.043	0.035
PLMM	0.101	0.041	0.033
GAN-HU	0.089	0.037	0.030
Meta-Spectral Net (Ours)	0.078	0.032	0.026

Table 4: Quantitative results on the Moffett dataset

Method	SAD	RMSE	RE
NMF	0.139	0.058	0.047
NMF-SV	0.127	0.052	0.043
PLMM	0.121	0.050	0.041
GAN-HU	0.105	0.045	0.037
Meta-Spectral Net (Ours)	0.091	0.038	0.031

Specifically, as shown in Table 2, on the Urban dataset, Meta-Spectral Net achieves the lowest values across all metrics, with an SAD of 0.082, RMSE of 0.036, and RE of 0.028, indicating significant improvements in both endmember extraction and abundance estimation accuracy. Similar trends are observed on the Samson dataset (Table 3), where our model yields an SAD of 0.078, RMSE of 0.032, and RE of 0.026, outperforming the second-best method by a clear margin. Notably, as presented in Table 4, the most substantial gains are evident on the Moffett dataset, which is characterized by pronounced spectral variability. Here, Meta-Spectral Net attains an SAD of 0.091, RMSE of 0.038, and RE of 0.031, underscoring its enhanced capability to handle complex spectral variations where traditional methods often falter.

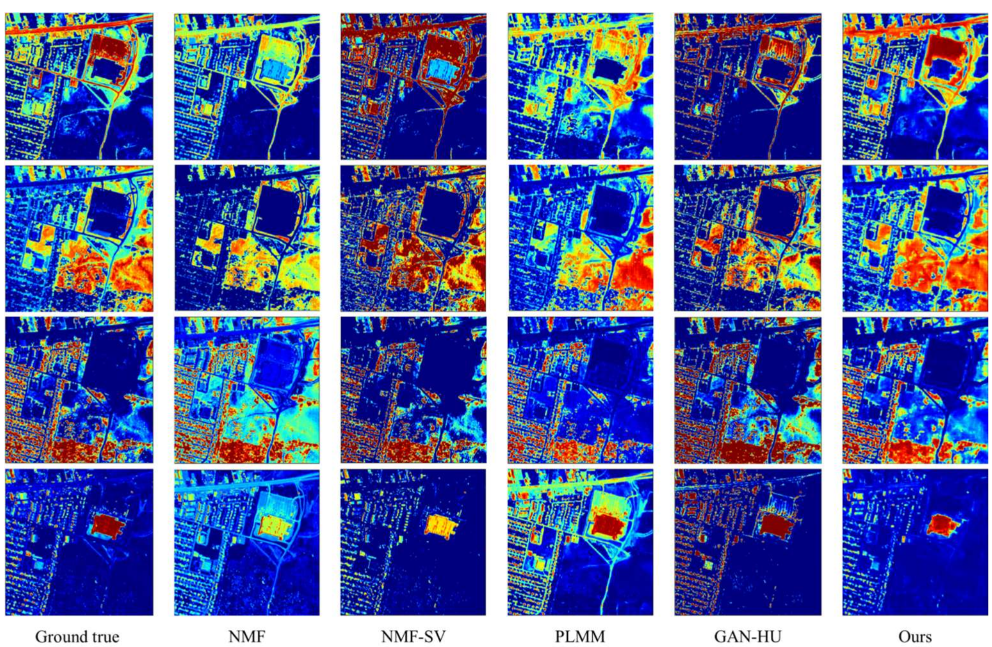

Figure 2: Abundance maps on the Urban dataset

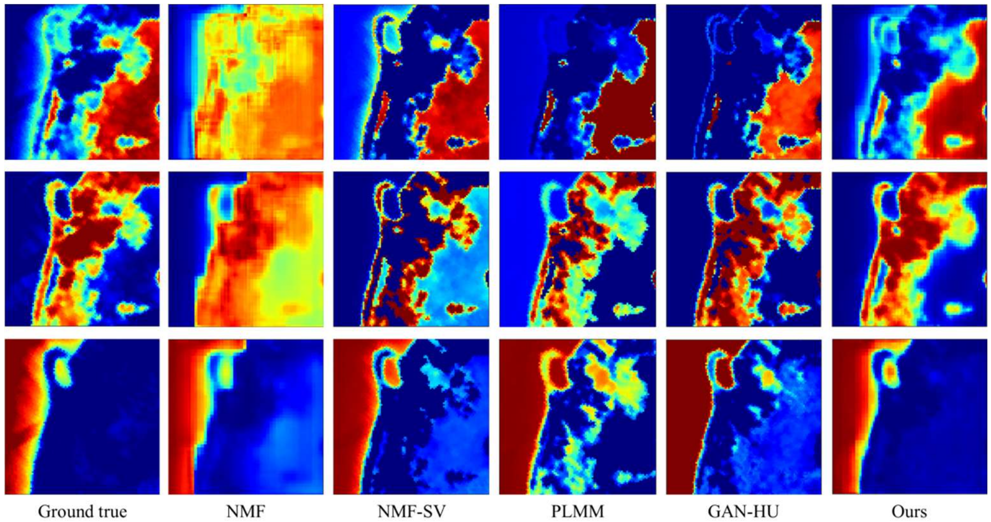

Figure 3: Abundance maps on the Samson dataset

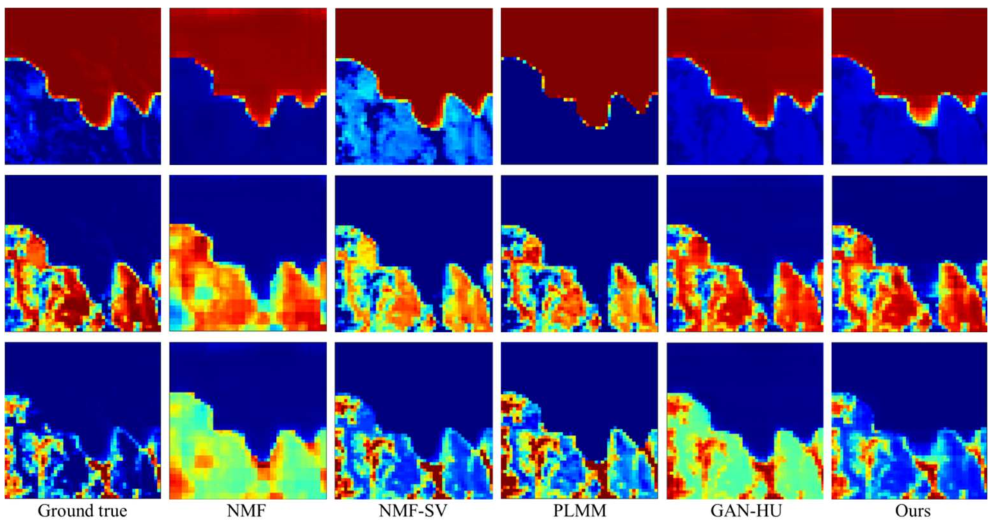

Figure 4: Abundance maps on the Moffett dataset

The superior quantitative results are further corroborated by qualitative analysis of the estimated abundance maps, visualized in Figures 2, 3, and 4. Visually, the abundance maps generated by Meta-Spectral Net exhibit smoother spatial distributions and are more physically plausible compared to those produced by baseline methods. In the Urban scene (Figure 2), the model shows a marked improvement in discriminating between the Asphalt and Roof endmembers, two materials that are frequently confused by conventional unmixing algorithms. For the Samson dataset (Figure 3), the proposed framework effectively suppresses noise artifacts and maintains sharper, more accurate boundaries around the Water region. In the challenging Moffett scenario (Figure 4), characterized by strong variability from coastal and aquatic influences, Meta-Spectral Net demonstrates remarkable robustness, producing cleaner and more distinct abundance maps for Vegetation and Water.

IV. C. Ablation Study

An ablation study was conducted to critically evaluate the contribution of each core component within the Meta-Spectral Net framework. The results, quantified in Table 5, clearly illustrate the importance of both the meta-learning mechanism and the spectral variability module.

Table 5: Ablation study on the Urban, Samson, and Moffett datasets

Model Variant	Urban (SAD)	Samson (SAD)	Moffett (SAD)	Avg. RMSE
without Meta-Learning	0.101	0.094	0.118	0.047
without Variability Module	0.097	0.089	0.112	0.044
Full Model (Ours)	0.082	0.078	0.091	0.036

Removing the meta-learning component ("Without Meta-Learning") results in a noticeable performance drop across all datasets, with the average SAD increasing to 0.104 and the RMSE rising to 0.047, highlighting its essential role in enabling rapid generalization to new conditions. Similarly, disabling the spectral variability module ("Without Variability Module"), which effectively reverts the model to using static endmembers, leads to severe performance degradation, particularly on the Moffett dataset (SAD of 0.112), confirming that explicitly modeling variability is crucial for handling real-world spectral changes. The full model ("Meta-Spectral Net") achieves the optimal balance, delivering the best performance and affirming that the synergistic combination of both components is fundamental to the framework's success.

IV. D. Discussion

The experimental findings lead to three principal conclusions. First, the proposed framework exhibits exceptional robustness to spectral variability, dynamically adapting to diverse environmental and acquisition conditions that typically challenge methods reliant on static endmember representations. Second, the meta-learning paradigm endows the model with strong generalization capabilities, allowing it to rapidly adapt to entirely new hyperspectral scenes with minimal fine-tuning, a significant advantage for practical applications. Finally, despite its advanced capabilities, the framework maintains computational efficiency comparable to existing methods, confirming its potential suitability for large-scale hyperspectral analysis tasks.

V. Conclusion and Future Work

In this paper, we presented Meta-Spectral Net, a novel meta-learning-based framework designed to address the critical challenge of spectral variability in hyperspectral unmixing. By integrating a task-driven meta-learning strategy with a dedicated spectral variability adaptation module, the proposed method enables rapid and effective adaptation of endmember representations under diverse and unseen imaging conditions. The framework was extensively evaluated on three widely-used hyperspectral datasets—Urban, Samson, and Moffett—demonstrating consistent and superior performance over both conventional linear and nonlinear unmixing models as well as recent deep learning-based approaches. Comprehensive quantitative evaluations using SAD, RMSE, and RE confirmed the effectiveness of our model, and ablation studies further validated the indispensable role of each core component.

The main contributions of this work are threefold. First, we introduced a meta-learning paradigm for hyperspectral unmixing, which facilitates fast adaptation of endmember characteristics across varying acquisition conditions, significantly enhancing model robustness. Second, we designed a variability-aware module that explicitly incorporates environmental and sensor-related factors into the endmember generation process, thereby improving the physical interpretability and accuracy of both abundance estimation and spectral reconstruction. Third, we provided extensive empirical validation across multiple benchmarks, establishing a new state-of-the-art performance in terms of reconstruction fidelity and generalization capability.

Despite these promising results, several directions remain open for future research. One limitation is the scalability to very large-scale hyperspectral scenes with high spatial-spectral resolutions; further optimizations in computational efficiency and memory usage would be necessary for such applications. Additionally, while the current model is purely data-driven, incorporating physical priors—such as radiative transfer models or atmospheric correction mechanisms—could strengthen both robustness and interpretability. Another important avenue is to improve cross-sensor generalization by explicitly modeling spectral response differences in the meta-learning framework. Finally, exploring few-shot or fully unsupervised adaptation strategies would help reduce the dependency on labeled data, making the approach more applicable in real-world scenarios where ground truth is scarce.

In conclusion, this study confirms the strong potential of combining meta-learning with explicit variability modeling to advance hyperspectral unmixing. We believe that Meta-Spectral Net provides a scalable and adaptive foundation for future research toward more physically consistent and operational unmixing systems.

Declaration of Conflicting Interests

The author(s) declared no potential conflicts of interest with respect to the research, author-ship, and/or publication of this article.

Data Sharing Agreement

The datasets used and/or analyzed during the current study are available from the corresponding author on reasonable request.

Funding

The author(s) received no financial support for the research, authorship, and/or publication of this article.

References

[1] Bioucas-Dias, J. M., Plaza, A., Dobigeon, N., Parente, M., Du, Q., Gader, P., & Chanussot, J. (2012). Hyperspectral unmixing overview: Geometrical, statistical, and sparse regression-based approaches. IEEE Journal of Selected Topics in Applied Earth Observations and Remote Sensing, 5(2), 354–379.

[2] Keshava, N., & Mustard, J. F. (2002). Spectral unmixing. IEEE Signal Processing Magazine, 19(1), 44–57.

[3] Plaza, A., Benediktsson, J. A., Boardman, J. W., Brazile, J., Bruzzone, L., Camps-Valls, G., ... & Trianni, G. (2009). Recent advances in techniques for hyperspectral image processing. Remote Sensing of Environment, 113, S110–S122.

[4] Iordache, M. D., Bioucas-Dias, J. M., & Plaza, A. (2011). Sparse unmixing of hyperspectral data. IEEE Transactions on Geoscience and Remote Sensing, 49(6), 2014–2039.

[5] Drumetz, L., Veganzones, M. A., & Chanussot, J. (2016). Variability of hyperspectral image endmembers: Recent advances and future prospects. IEEE Geoscience and Remote Sensing Magazine, 4(2), 29–46.

[6] Zare, A., & Ho, K. C. (2014). Endmember variability in hyperspectral analysis: Addressing spectral variability during spectral unmixing. IEEE Signal Processing Magazine, 31(1), 95–104.

[7] Thouvenin, P. A., Drumetz, L., & Chanussot, J. (2016). Hyperspectral unmixing with spectral variability using a perturbed linear mixing model. IEEE Transactions on Signal Processing, 64(2), 525–538.

[8] Drumetz, L., Meyer, T., Chanussot, J., Bertozzi, A. L., & Guillemot, C. (2019). Linear–quadratic mixing model for hyperspectral unmixing: Existence and uniqueness. IEEE Transactions on Image Processing, 28(2), 862–875.

[9] Heylen, R., Parente, M., & Gader, P. (2014). A review of nonlinear hyperspectral unmixing methods. IEEE Journal of Selected Topics in Applied Earth Observations and Remote Sensing, 7(6), 1844–1868.

[10] Halimi, A., Altmann, Y., Dobigeon, N., & Tourneret, J. Y. (2015). Nonlinear unmixing of hyperspectral images using a generalized bilinear model. IEEE Transactions on Geoscience and Remote Sensing, 53(5), 2252–2263.

[11] Zhang, L., Zhang, L., & Du, B. (2018). Deep learning for remote sensing data: A technical tutorial on the state of the art. IEEE Geoscience and Remote Sensing Magazine, 6(2), 22–40.

[12] Palsson, F., Sveinsson, J. R., & Ulfarsson, M. O. (2018). Endmember variability in hyperspectral unmixing: A new approach using autoencoders. IEEE International Geoscience and Remote Sensing Symposium (IGARSS), 2018, 2083–2086.

[13] Jia, S., & Qian, Y. (2007). Constrained nonnegative matrix factorization for hyperspectral unmixing. IEEE Transactions on Geoscience and Remote Sensing, 45(1), 86–97.

[14] Finn, C., Abbeel, P., & Levine, S. (2017). Model-agnostic meta-learning for fast adaptation of deep networks. Proceedings of the 34th International Conference on Machine Learning (ICML), 70, 1126–1135.

[15] Hospedales, T. M., Antoniou, A., Micaelli, P., & Storkey, A. J. (2021). Meta-learning in neural networks: A survey. IEEE Transactions on Pattern Analysis and Machine Intelligence, 44(9), 5149–5169.

[16] D. D. Lee and H. S. Seung, "Algorithms for non-negative matrix factorization," in Advances in Neural Information Processing Systems, vol. 13, 2001.

[17] R. Heylen, M. Parente, and P. Gader, "A review of nonlinear hyperspectral unmixing methods," IEEE Journal of Selected Topics in Applied Earth Observations and Remote Sensing, vol. 7, no. 6, pp. 1844-1868, June 2014.

[18] Z. Wei, J. Wang, N. Akhtar, and Y. Li, "GAN-Based Hyperspectral Unmixing," in IEEE Geoscience and Remote Sensing Letters, vol. 19, pp. 1-5, 2022, Art no. 8023305.